Available online at www.sciencedirect.com
ScienceDirect
Mendeleev Commun., 2017, **27**, 512–514

Mendeleev Communications

Silica-supported iron oxide nanoparticles: unexpected catalytic activity in hydrogenation of phenylacetylene

Anastasiya A. Shesterkina,*[a] Elena V. Shuvalova,[a] Elena A. Redina,[a] Olga A. Kirichenko,[a] Olga P. Tkachenko,[a] Igor V. Mishin[a] and Leonid M. Kustov[a,b]

[a] *N. D. Zelinsky Institute of Organic Chemistry, Russian Academy of Sciences, 119991 Moscow, Russian Federation. Fax: +7 499 135 5328; e-mail: anastasiia.strelkova@mail.ru*
[b] *Department of Chemistry, M. V. Lomonosov Moscow State University, 119991 Moscow, Russian Federation*

DOI: 10.1016/j.mencom.2017.09.028

Hydrogenation of phenylacetylene in liquid phase (100–150 °C, 6–20 bar H_2) over FeO_x/SiO_2 catalysts prepared by thermal decomposition of ammonium trioxalatoferrate affords styrene with selectivities 70–80% depending on temperature and pressure.

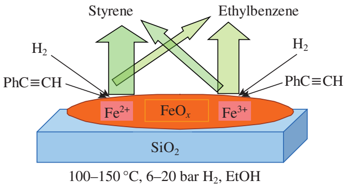

The development of efficient and environmentally safe catalytic systems is a topical problem of up-to-date catalysis. The abundance, low cost and low toxicity of iron oxides make their use in catalysis highly sustainable and preferable as compared to the commonly used Pd, Pt, Ru, Rh, and Ni catalysts of hydrogenation. Generally, iron-based catalysts have been applied at high temperatures and high pressures for large-scale fuel and platform chemical production (the Haber–Bosch process, the water–gas shift and the Fischer–Tropsch reactions) as well as for organic synthesis.[1–4] However, only a handful of iron catalysts have been developed for selective hydrogenation under relatively mild conditions.[2–8] Recently, Fe^0 nanoparticles of 1–5 nm in diameter were reported to catalyze hydrogenation of olefins and alkynes in organic solvents, while no hydrogenation of aromatic ring was observed.[9–10] A limitation of the use of such Fe^0 nanoparticles resides in their sensitivity towards oxidation, the complicated preparation process and impossibility of separation even magnetically. The Fe^0 nanoparticles were synthesized from specific expensive reagents under water- and oxygen-free conditions. The core-shell iron (iron oxide) materials prepared in water-containing solutions using common Fe salt and reducing agent, as well as the commercial iron core-shell nanoparticle materials are more stable to water and air.[11] The powder of these materials comprising the chains of larger particles consisting of Fe^0 core (diameter of 44 nm) and a Fe oxide shell (thickness of 6 nm) can be magnetically separated from the reaction medium. Such catalysts are active and strictly selective for alkene and alkyne hydrogenation in the presence of carbonyl and aromatic groups, suggesting that the occurrence of an iron oxide shell is not an obstacle to the catalytic activity at 80 °C and 40 bar H_2.

In view of the fact that smaller Fe^0 nanoparticles exhibited the catalytic activity at lower temperatures and H_2 pressures (25 °C and 10–20 bar),[9,10] it seems important to find the way of their stabilization *via* deposition on the surface of a shaped support. The modification of Fe nanoparticles with a silicone polymer affords a nanocomposite containing particles with a size of 2–3 nm with the Fe^0–FeO_x core-shell structure.[12] These hybrid systems modified with metal nanoparticles seem promising for catalysis. Heterogeneous catalysts in the form of shaped bodies can be efficiently separated and used in a continuous-flow process instead of periodic batch process (*cf.* ref. 13). However, the preparation of Fe_3O_4 (6 nm)/alumina catalyst[13] is very complex, and its activity depends on the nature of silica support. The supported Fe^0 nanoparticles have been prepared using common procedure by reduction of silica-deposited Fe precursor at 500 °C in a hydrogen flow.[14,15] These 50% Fe/SiO_2 materials are active and selective for the partial hydrogenation of phenylacetylene (PA) at 60 °C and H_2 pressure 10 bar, while the hydrogenation rates are low, perhaps, due to the large (~17 nm) particle size.

Previously,[16–18] we prepared materials comprising iron oxide nanoparticles on the alumina and silica supports by means of low temperature decomposition of ammonium trioxalatoferrate salt in air.[19] Herein, we tested them in liquid-phase hydrogenation of PA,[†] which is commonly used as a model reaction in the studies on the catalytic activity of materials in hydrogenation of alkynes under mild conditions due to its commercial importance.[10,14,20,21]

Hydrogenation of PA over the FeO_x/HS samples started at 100–105 °C giving styrene and ethylbenzene at the 99% carbon balance. The complete conversion occurred at 105 °C in 2–5 h depending on the temperature of preliminary calcination of the

---

[†] The FeO_x/SiO_2 materials were prepared by incipient wetness impregnation of a silica support with a saturated aqueous solution of $(NH_4)_3[Fe(C_2O_4)_3]\cdot 3H_2O$ (pure, 98%, Acros Organics). The granulated commercial silica supports with a high specific (HS) surface area (S = = 300 $m^2 g^{-1}$, average pore width 12 nm, Russia) and a low specific (LS) surface area (S = 105 $m^2 g^{-1}$, average pore width 36 nm, Khimmed, Russia) were used. The impregnated samples were dried at 60 °C in an oven and then calcined at 250–500 °C in air to decompose the precursor.[20–22] The reference sample α-Fe_2O_3 with S_{BET} = 90 $m^2 g^{-1}$ was prepared by decomposition of $(NH_4)_3[Fe(C_2O_4)_3]\cdot 3H_2O$ at 500 °C in air, its phase composition was confirmed with XRD analysis.

The samples were characterized by TEM, XRD analysis and DRIFT spectroscopy of adsorbed CO using the described procedures.[22,23] The samples morphology was studied using a Hitachi HT7700 transmission electron microscope. Images were acquired in the bright-field TEM mode at the 100 kV accelerating voltage. Before measurements, the samples were deposited on 3 mm carbon-coated copper grids from isopropanol suspension. Target-oriented approach was used for the optimization of the analytical measurements.[25]

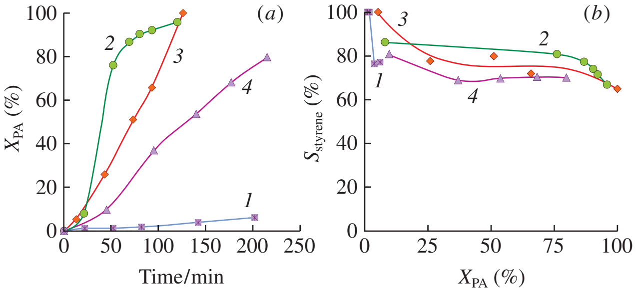

Figure 1 (*a*) Time dependence of the PA conversion and (*b*) styrene selectivity *vs.* PA conversion over (*1*) α-Fe_2O_3 and the FeO_x/HS sample calcined at (*2*) 250, (*3*) 400 and (*4*) 500 °C. Reaction conditions: $C_{0\,PA}$ = = 0.13 M; $n_{PA}:n_{Fe}$ = 12; *T* = 105 °C; p_{H_2} = 13 bar.

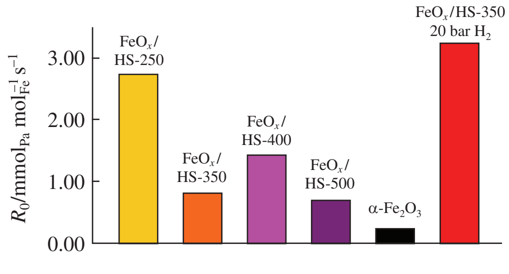

Figure 2 Initial rate of PA hydrogenation for the FeO_x/HS sample calcined at 250, 350, 400 and 500 °C and α-Fe_2O_3. Reaction conditions: $C_{0\,PA}$ = 0.13 M; *T* = 105 °C; p_{H_2} = 13 bar.

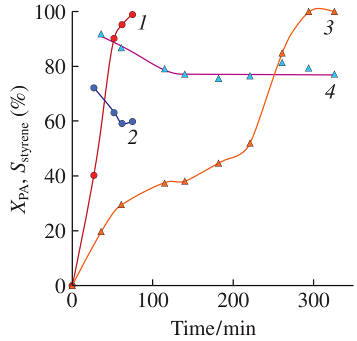

Figure 3 Time dependence of (*1*, *3*) PA conversion and (*2*, *4*) styrene selectivity over the FeO_x/HS sample calcined at 350 °C. Reaction conditions: $C_{0\,PA}$ = 0.15 M; $n_{PA}:n_{Fe}$ = 10; *T* = 105 °C; p_{H_2} = 20 (*1*, *2*) or 13 bar (*3*, *4*).

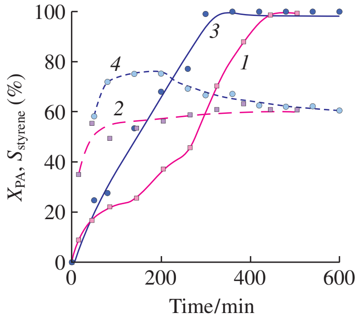

Figure 4 Time dependence of the (*1*, *3*) PA conversion and (*2*, *4*) selectivity to styrene over the samples (*1*, *2*) FeO_x/HS calcined at 350 °C and (*3*, *4*) FeO_x/LS reduced in H_2 at 350 °C. Reaction conditions: $C_{0\,PA}$ = 0.13 M; $n_{PA}:n_{Fe}$ = 15; *T* = 110 °C; p_{H_2} = 13 bar.

sample [Figure 1(*a*)]. The selectivity to styrene depended on the PA conversion as well as on the calcination temperature of the samples [Figure 1(*b*)]. The best selectivity reached 80% for 75% PA conversion at p_{H_2} = 13 bar over the sample calcined at 250 °C, whereas it decreased to 60–65% when approaching the full PA conversion.

The highest initial rates of PA hydrogenation were observed for the material calcined at 250 °C (Figure 2). The relatively low initial rate for the samples calcined at 350 °C seems to be strange, however, these results were highly reproducible. The catalytic activity of the bulk α-Fe_2O_3 sample was very low as compared with the silica-supported iron oxide materials [Figures 1(*a*), 2].

The H_2 pressure affected the catalytic activity which considerably increased at 20 bar as compared with that at 13 bar, for example, over the FeO_x/HS sample calcined at 350 °C (Figures 2, 3). It should be mentioned that induction period was observed when the reaction was performed at lower H_2 pressure of 6 bar. This feature demonstrates the generation of the active sites that performed the hydrogenation of a triple bond only in direct contact with the reaction mixture and H_2. The induction period disappeared at the higher H_2 pressure of 13–20 bar. The sample calcined at 350 °C seems to contain two iron oxide phases. The first one is Fe_3O_4 as the product of thermal decomposition of ammonium trioxalatoferrate at 250 °C, and another one is Fe_2O_3, the product of its oxidation at higher temperatures.[16–19] These phases are likely to exhibit different rates of initial reduction under reaction conditions, which results in S-shaped conversion curves for the samples calcined at 350 °C.

Apparently, the sample surface is reduced *in situ* before the reaction starts. It should be pointed out that preliminary reduction to Fe_3O_4 in a hydrogen flow at 350 °C (conditions based on data from ref. 18) resulted in a more active catalyst FeO_x/LS (LS is low surface) compared to FeO_x/HS calcined at 350 °C with a close selectivity (67 and 60%, respectively) at the complete PA conversion (Figure 4).

The obtained data revealed that hydrogen consumptions occurred only until the complete PA conversion to styrene and ethylbenzene. No further styrene hydrogenation was observed (Figure 4), perhaps, due to very weak adsorption of a double bond on the surface sites of the samples. This fact allows us to suppose that PA hydrogenation to styrene and to ethylbenzene proceeded as parallel reactions on different surface sites.

The main results obtained in a mini-autoclave are summarized in Table 1. The PA conversion was similar for the samples on both supports at 110 °C, while at 150 °C it was higher for the sample prepared using the HS silica. The selectivity to styrene decreased with the reaction temperature. It should be mentioned

Table 1 Hydrogenation of PA over the FeO_x/SiO_2 samples and the SiO_2 supports calcined at 350 °C.[a]

Sample	*T*/°C	τ/h	X_{PA} (%)	$S_{styrene}$ (%)	$S_{ethylbenzene}$ (%)
FeO_x/HS	110	4	13	76	24
	150	2	97	41	59
HS-SiO_2	150	2	6	81	13
FeO_x/LS	110	4	10	87	13
	150	3	16	59	41
LS-SiO_2	150	3	5	83	12

[a] Reaction conditions: mini-autoclave, C_{PA} = 0.15 M, $n_{PA}:n_{Fe}$ = 5; $C_{C_{20}H_{42}}$ = = 0.19 M; p_{H_2} = 10 bar.

The catalytic properties of FeO_x/SiO_2 samples were studied in the liquid phase hydrogenation in the batch mode using a lab-constructed mini-autoclave glass reactor (5 ml), as well as a larger autoclave (100 ml) fitted with a glass reactor and a probe valve. The reaction conditions were as follows: the 0.13–0.15 M PA solution in ethanol, the H_2 pressure 6–20 bar, 100–150 °C, the molar ratio PA : Fe = 5–15. The reaction products were identified by GC analysis[24,25] with undecane as an internal standard (0.19 M) that was introduced in the initial reaction mixture. Only styrene and ethylbenzene were formed as the reaction products. The time dependence of the PA conversion and selectivity to styrene was studied. The catalytic activity was evaluated by the initial rate of PA hydrogenation referred to the molar amount of iron.

that some PA hydrogenation proceeded over the Fe-free supports at 150 °C when an incomplete C balance (94–95%) indicated formation of some other products in such a process.

The TEM images of the FeO_x/HS samples calcined in air at 250–350 °C (Figure S1, see Online Supplementary Materials) provide evidence for numerous isolated nanoparticles of the size 1–4 nm that are clearly recognized as dark features with almost a spherical or semispherical shape. In addition to isolated nanoparticles, their aggregates of the size 10–20 nm can be found in the images of the FeO_x/HS sample after calcination. Only slight changes in the particle size were observed when the calcination temperature of the sample was raised from 250 up to 400 °C. In the TEM images of the FeO_x/LS sample calcined in air at 350 °C, the seldom crystallites of the size 10–20 nm were observed in addition to the above mentioned nanoparticles and aggregates (Figure S1). The silica-supported nanoparticles in all samples, even calcined in air at 500 °C, were XRD amorphous, while the diffraction pattern of the bulk iron oxide sample exhibited the reflections of the α-Fe_2O_3 phase with corresponding intensities. The α-Fe_2O_3 sample consisted mostly of the isolated nanoparticles of the size 10–20 nm.

DRIFT spectroscopic studies with adsorbed CO as a test molecule revealed the presence of Fe^{2+} ions on the surface of the samples calcined at 250 and 350 °C. DRIFT spectra recorded after CO adsorption for 10 min on the samples evacuated at 350 °C for 2 h exhibited a single intense band at 2164 cm^{-1} (Figure 5), whereas no bands were detected when the samples were evacuated at 250 °C. The band at 2164 cm^{-1} was also observed in the spectra of the sample calcined at 400 °C. The intensity of this band decreased on heating to calcination temperature. Exposition to CO for 17 h caused no changes of the band, and it disappeared after evacuation at room temperature for 30 min. This band can be attributed to the linear form of CO adsorption on Fe^{2+} sites.[27] A very weak intensity of this band indicates a small amount of Fe^{2+} in the sample after calcination at 400 °C in air, supposing the high extent of oxidation to Fe_2O_3. One more band at 2353 cm^{-1} arises in the spectra of the sample calcined at 400 °C, and the intensity of this band increases considerably after treatment with CO for 17 h (Figure 5). The band disappeared after evacuation at room temperature. It is characteristic of adsorbed CO_2 and indicates CO oxidation with lattice oxygen on Fe^{3+} sites that are thereby reduced to Fe^{2+} ions.[27]

The presence of Fe^{2+} sites on the surface of iron oxide particles formed after decomposition of supported ammonium trioxalatoferrate at 250 °C, as well as further appearance and domination of Fe^{3+} sites after calcination at 400 °C, are in agreement with the data on thermal analysis of supported ammonium trioxalatoferrate.[18,19] Thermal analysis clearly indicated the oxidation process at 250–350 °C occurring after the decomposition.

In summary, iron oxides have been deposited on the surface of the silica supports as the finely dispersed isolated and aggregated nanoparticles (smaller than 5 nm) using a very simple, waste-free and environmentally safe procedure. These nanoparticles catalyze hydrogenation of the triple C≡C bond in PA in the liquid phase under relatively mild conditions. The catalyst herein obtained is superior to its analogues reported previously.[9–11,14,15]

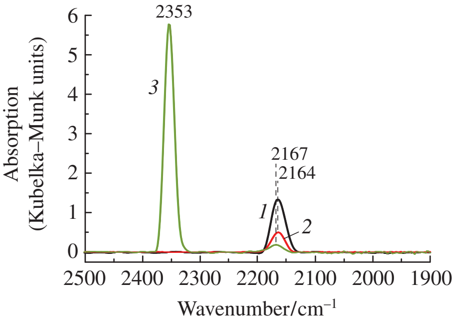

Figure 5 DRIFT spectra recorded after CO adsorption for 17 h on the FeO_x/HS samples calcined at (*1*) 250, (*2*) 350 and (*3*) 400 °C.

Electron microscopy characterization was performed in the Department of Structural Studies of the N. D. Zelinsky Institute of Organic Chemistry, Russian Academy of Sciences.

This work was supported by the Russian Science Foundation (project no. 14-50-00126).

Online Supplementary Materials

Supplementary data associated with this article can be found in the online version at doi: 10.1016/j.mencom.2017.09.028.

References

1 J. H. Docherty and S. P. Thomas, in *Sustainable Catalysis: With Non-endangered Metals*, Part 1, ed. M. North, RCS Green Chemistry Series, 2015, pp. 344–372.
2 A. Baeza, G. Guillena and D. J. Ramón, *ChemCatChem*, 2016, **8**, 49.
3 R. Hudson, Y. Feng, R. S. Varma and A. Moores, *Green Chem*., 2014, **16**, 4493.
4 A. Welther and A. J. von Wangelin, *Curr. Org. Chem*., 2013, **17**, 326.
5 S. Gaillard and J.-L. Renaud, *ChemSusChem*, 2008, **1**, 505.
6 K. Junge, K. Schröder and M. Beller, *Chem. Commun*., 2011, **47**, 4849.
7 R. V. Jagadeesh, A.-E. Surkus, H. Junge, M.-M. Pohl, J. Radnik, J. Rabeah, H. Huan, V. Schünemann, A. Brückner and M. Beller, *Science*, 2013, **342**, 1073.
8 A. V. Erokhin, E. S. Lokteva, A. Ye. Yermakov, D. W. Boukhvalov, K. I. Maslakov, E. V. Golubina and M. A. Uimin, *Carbon*, 2014, **74**, 291.
9 P.-H. Phua, L. Lefort, J. A. F. Boogers, M. Tristany and J. G. de Vries, *Chem. Commun.*, 2009, **45**, 3747.
10 V. Kelsen, B. Wendt, S. Werkmeister, K. Junge, M. Beller and B. Chaudret, *Chem. Commun*., 2013, **49**, 3416.
11 R. Hudson, A. Rivière, C. M. Cirtiu, K. L. Luska and A. Moores, *Chem. Commun.*, 2012, **48**, 3360.
12 A. Yu. Vasil'kov, D. A. Migulin, A. V. Naumkin, O. A. Belyakova, Ya. V. Zubavichus, S. S. Abramchuk, Yu. V. Maksimov, S. V. Novichikhin and A. M. Muzafarov, *Mendeleev Commun*., 2016, **26**, 187.
13 M. M. Moghaddam, B. Pieber, T. Glasnov and C. O. Kappe, *ChemSusChem*, 2014, **7**, 3122.
14 Y. Nitta, S. Matsugi and T. Imanaka, *Catal. Lett*., 1990, **5**, 67.
15 Y. Nitta, Y. Hiramatsu, Y. Okamoto and T. Imanaka, *Studies Surf. Sci. Catal.*, 1993, **75**, 2333.
16 O. A. Kirichenko, V. A. Ushakov and V. A. Poluboyarov, *React. Kinet. Catal. Lett*., 1993, **51**, 167.
17 L. M. Kustov, S. R. Al-Abed, J. Virkutyte, O. A. Kirichenko, E. V. Shuvalova, G. I. Kapustin, I. V. Mishin, V. D. Nissenbaum, O. P. Tkachenko and E. D. Finashina, *Pure Appl. Chem.*, 2014, **86**, 1141.
18 O. A. Kirichenko, G. I. Kapustin, V. D. Nissenbaum, I. V. Mishin and L. M. Kustov, *J. Therm. Anal. Calorim*., 2014, **118**, 749.
19 O. A. Kirichenko, V. D. Nissenbaum, G. I. Kapustin and L. M. Kustov, *Termochim. Acta*, 2009, **494**, 35.
20 G. Petrucci, W. Oberhauser, M. Bartoli, G. Giachi, M. Frediani, E. Passaglia, L. Capozzoli and L. Rosi, *Appl. Catal. A*, 2014, **469**, 132.
21 J. Hu, Z. Zhou, R. Zhang, L. Li and Z. Cheng, *J. Mol. Catal. A*, 2014, **381**, 61.
22 O. A. Kirichenko, N. A. Davshan, E. A. Redina, G. I. Kapustin, I. V. Mishin, O. P. Tkachenko, A. V. Kucherov and L. M. Kustov, *Chem. Eng. J*., 2016, **292**, 62.
23 O. A. Kirichenko, G. I. Kapustin, O. P. Tkachenko, V. D. Nissenbaum, I. V. Mishin, N. A. Davshan, E. A. Redina and L. M. Kustov, *Mater. Res. Bull*., 2016, **80**, 139.
24 V. V. Kachala, L. L. Khemchyan, A. S. Kashin, N. V. Orlov, A. A. Grachev, S. S. Zalesskiy and V. P. Ananikov, *Russ. Chem. Rev*., 2013, **82**, 648.
25 A. A. Shesterkina, L. M. Kozlova, O. A. Kirichenko, G. I. Kapustin, I. V. Mishin and L. M. Kustov, *Russ. Chem. Bull., Int. Ed*., 2016, **65**, 432 (*Izv. Akad. Nauk, Ser. Khim*., 2016, 432).
26 A. A. Shesterkina, O. A. Kirichenko, L. M. Kozlova, G. I. Kapustin, I. V. Mishin, A. A. Strelkova and L. M. Kustov, *Mendeleev Commun*., 2016, **26**, 228.
27 A. Davydov, *Molecular Spectroscopy of Oxide Catalyst Surfaces*, Wiley, London, 2003.

Received: 14th December 2016; Com. 16/5124